RSC Advances

ROYAL SOCIETY OF CHEMISTRY

www.rsc.org/advances

Graphical abstract

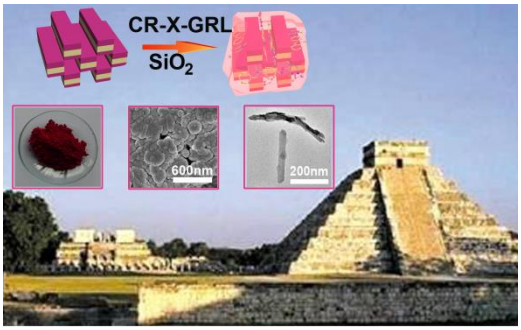

RSC Advances

RSCPublishing

ARTICLE

Facile preparation of stable palygorskite/cationic red X-GRL@SiO_2 "Maya Red" pigments

Cite this: DOI: 10.1039/x0xx00000x

Received 00th January 2012,
Accepted 00th January 2012

DOI: 10.1039/x0xx00000x

www.rsc.org/

Ling Fan,[a, b] Yujie Zhang,[a, b, c] Junping Zhang,[*a, b] and Aiqin Wang[a, b]

Inspired by Maya Blue, we report fabrication of stable "Maya Red" pigments with purple-red hue by adsorption of cationic red X-GRL (CR-X-GRL) onto palygorskite (PAL), which is followed by hydrolysis and polycondensation of tetraethoxysilane (TEOS) via a modified Stöber method to form a layer of SiO_2. The parameters influencing the adsorption of CR-X-GRL onto PAL (e.g., $m_{CR\text{-}X\text{-}GRL}/m_{PAL}$ and the ball milling time) and polycondensation of TEOS (e.g., concentrations of TEOS and ammonia, and volume ratio of ethanol to water) were investigated by using stability of the pigment as the probe. The CR-X-GRL content in the PAL/CR-X-GRL pigments can be as high as 12%, which is higher than all the state-of-the-art Maya Blue-like pigments. Since the stability of the PAL/CR-X-GRL pigments is not very high, a layer of SiO_2 was introduced to further improve the stability. The SEM, TEM, FTIR and BET data prove the presence of silica on the surface of the PAL/CR-X-GRL pigment. The PAL/CR-X-GRL@SiO_2 "Maya Red" pigments show excellent chemical (1M HCl, 1M NaOH and ethanol), thermal and UV stability.

Introduction

Nowadays, organic/inorganic hybrid materials with excellent properties are of great interests in various academic and industrial fields.[1] Incorporation of small molecules by adsorption in meso- and micro-porous materials is a frequently employed strategy to fabricate materials with novel properties.[2, 3] The famous Pre-Columbian Maya Blue pigment, an ancient nanostructured material discovered by Merwin in 1931, is a beautiful example of remarkable man-made hybrid materials.[4-6] As a robust hybrid pigment of palygorskite (PAL) and indigo, it was widely used in mural paintings of Mayan ceremonial sites in the Yucatan and in many ceramic pieces.[7, 8] PAL, a phyllosilicate microporous clay mineral with large specific surface area, is renowned for its ability to adsorb ionic species, especially the cationic organic compounds. The whole adsorption process is mainly controlled by electrostatic attraction and/or cation exchange.[9, 10]

A particularly fascinating property of Maya Blue is that it doesn't fade despite in the environment of harsh humidity and high temperature for thousands of years. Thus, Maya Blue has attracted much attention of researchers in the fields of material, chemistry and archaeology in the past decades.[11-13]

On the one hand, researchers have tried various techniques to reveal why Maya Blue is so stable. The indigo molecules may penetrate into the tunnels of PAL,[14-18] or be adsorbed onto the grooves[8], or block the entrances of the channels.[19, 20] The iron, aluminum and magnesium ions should have some influences on the interaction between indigo and PAL.[16, 21] Some authors claimed that the zeolitic water of PAL plays an important role in forming the very stable Maya Blue pigment.[16, 17] Different forms of indigo including reduced and oxidized indigo can be found in the Maya Blue pigment.[22, 23] The interaction between indigo and PAL is complex, including hydrogen bonding between C=O and N–H of the dye with the edge silanols of PAL,[20, 24] hydrogen bonding between carbonyls of indigo and structural water of PAL,[14, 15, 24] direct bonding between the octahedral Mg^{2+} and Al^{3+} cations of PAL and the dye molecules,[20] as well as specific bonding to Al^{3+} substituted Si^{4+} sites in tetrahedral centers.[19, 25]

On the other hand, many methods have been used to fabricate stable Maya Blue-like pigments from the perspective of clays and organic dyes. Clays including zeolite, sepiolite and PAL, and dyes including indigo, methyl red and Sudan red have been used for preparing synthetic Maya Blue-like pigments.[7, 23, 26-29] However, the stability of Maya Blue-like pigments remains to be improved.

Silica, an inorganic matrix, has several advantages in the spectral region of interest because of their low optical losses, good mechanical properties (high strength, stiffness, hardness and abrasion resistance) and long-term environmental stability.[30] Silica nanomaterials have a broad range of applications including solid supports and entrapping matrices due to their unique features such as little absorption in the

UV-Vis region and low toxicity, etc.[31-36] Additionally, polar dye molecules could be easily entrapped in the negatively charged silica matrix via electrostatic attraction.[35] Silica-coated materials show the colour of the dyes themselves since silica is optically transparent.[37] Leakage of dye molecules from silica is negligible because of the strong electrostatic attraction between the positively charged dye and the negatively charged silica.[35] The silica matrix serves as a protective shell or dye isolator, limiting the effect of the outside environment (such as oxygen, certain solvents, and soluble species in buffer solutions) on the dye contained in the nanoparticles.

Here we report fabrication of stable "Maya Red" pigments with a purple-red hue by adsorption of cationic red X-GRL (CR-X-GRL) onto PAL, which is followed by hydrolysis and polycondensation of tetraethoxysilane (TEOS) via a modified Stöber method to form a layer of SiO_2. The parameters influencing the adsorption of CR-X-GRL onto PAL (e.g., weight ratio of CR-X-GRL to PAL ($m_{CR\text{-}X\text{-}GRL}/m_{PAL}$) and the ball milling time) and polycondensation of TEOS (e.g., concentrations of TEOS and ammonia, and volume ratio of ethanol to water ($V_{ethanol}/V_{H2O}$) were investigated by using stability of the pigment as the probe. The aim of this work is to find a new way to prepare stable Maya Blue-like pigments.

Experimental section

Materials

Natural PAL, obtained from Xuyi, Jiangsu Province, China, was crushed and purified by 2% H_2SO_4 to remove quartz and other impurities, such as carbonates, etc. The purified PAL was filtered by passing through a 180-mesh sieve. CR-X-GRL was provided by Binhai Torch Technology, Co., Ltd. TEOS was purchased from Gelest. All chemicals were used as received without further purification. Deionized water was used for all the experiments and tests.

Synthesis of PAL/CR-X-GRL pigments

The PAL/CR-X-GRL pigments were prepared according to the following procedure. 2.0 g of PAL was dispersed in 20 mL of concentrated CR-X-GRL ethanol solution. The mixtures have an $m_{CR\text{-}X\text{-}GRL}/m_{PAL}$ of 4% ~ 20% (w/w) by varying the concentration of CR-X-GRL. The mixtures were shaken in a thermostatic shaker (THZ-98A, Chincan, Zhejiang, China) at 30 °C and 200 rpm for 4 h to accomplish the adsorption of CR-X-GRL onto PAL. The mixtures were vacuum filtered, and then the filter cakes were dried in an oven at 60 °C for 4 h. For the ball-milled samples, the samples (1.0 g) were milled in an agate ball mill at 100 rpm for 0-240 minutes.

Synthesis of PAL/CR-X-GRL@SiO_2 pigments

The PAL/CR-X-GRL@SiO_2 pigments were prepared by hydrolysis and polycondensation of TEOS via a modified Stöber method. 1.0 g of PAL/CR-X-GRL pigment was charged into 40 mL of ethanol containing 0 ~ 1.5 mL of TEOS and 0.1 ~ 0.5 mL of 25% ammonia at 50 °C. The suspension was ultrasonicated for 10 min, and then a proper amount of water was injected quickly into the solution under ultrasonication. The total volume of ethanol and water is 50 mL, and the $V_{ethanol}/V_{H2O}$ is in the range of 47.25/2.5 to 35/15. After kept at 70 °C for 48 h, the PAL/CR-X-GRL@SiO_2 pigment was washed with 20 mL of ethanol for 3 times and dried in an oven at 60 °C.

Stability tests

For the chemical stability tests, 0.2 g of sample was charged into 8 mL of anhydrous ethanol, 1 M NaOH or 1 M HCl under vigorous stirring in a vial. The suspension was shaken in a thermostatic shaker (THZ-98A, Chincan, Zhejiang, China) at 30 °C and 120 rpm for 24 h, and then centrifugated at 5000 rpm for 10 min. The released dye in the supernatant was determined using a UV-Vis spectrophotometer (Specord 200, Analytik Jena AG). A higher concentration of dye in the supernatant means lower stability of the pigment. The UV accelerated weathering tests were carried out according to the following procedure. Firstly, aluminum foils were cleaned by washing with ethanol, acetone and distilled water in turn, and then dried under a nitrogen flow. A spray coating dispersion was prepared by adding 0.4 g of the sample in 40 mL of acetone. Then, the dispersion was spray coated onto a vertically placed aluminum foil using an airbrush (INFINITY 2 in 1, Harder & Steenbeck, Germany) at a nitrogen flow rate of 150 L/h with a distance of 6 cm. Finally, the coated samples were put into an UV Accelerated Weathering Tester (ZN-P, Xinlang, Shanghai, China) with at 50 w/m^2 and 60 °C for a period of time. Thermal stability of samples was carried out using a STA 6000 simultaneous thermal analyzer (PerkinElmer Instrument Co., Ltd. USA). The temperature program was 10 °C /min from 20 to 800 °C under constant N_2 atmosphere with a flow rate of 20 mL/min. The thermal stability tests were also performed in an oven under air atmosphere at 60 °C, 140 °C and 160 °C for 12 h.

Characterization

FTIR spectra of samples were recorded on a Thermo Nicolet NEXUS TM spectrophotometer using KBr pellets. The micrographs of the samples were taken using a field emission scanning electron microscope (SEM, JSM-6701F, JEOL) and a field emission transmission electron microscope (TEM, JEM-1200EX, FEI). Before SEM observation, all samples were fixed on aluminum stubs and coated with gold (~ 7 nm). For TEM observation, the samples were prepared as follows. A drop of the samples in ethanol was put on a copper grid and dried in the open atmosphere. The energy dispersive X-ray analysis (EDX) was done on an attachment to TEM. The pore volume and surface area of the samples were determined by N_2 sorption isotherm and application of the BET theory. The instrument used was a micromeritics ASAP 2020 and the supplied software was used to manipulate the experimental data. The XRD patterns of samples were obtained using a Philips X-ray diffraction instrument with filtered Cu Kα radiation (n = 1.5418 Å) operated at 40 kV and 40 mA. The XRD patterns were recorded from 3 to 70° at a scanning speed of 3°/min.

Results and discussion

Design of PAL/CR-X-GRL@SiO_2 pigments

The PAL/CR-X-GRL@SiO_2 "Maya Red" pigments were fabricated by adsorption of organic CR-X-GRL on PAL in aqueous solutions, and then modified by polycondensation of TEOS (Scheme 1). The effects of various parameters in the adsorption of CR-X-GRL on PAL (*e.g.*, $m_{CR\text{-}X\text{-}GRL}/m_{PAL}$ and the ball milling time) and the coating of PAL/CR-X-GRL with SiO_2 (*e.g.*, concentrations of TEOS and ammonia, and $V_{ethanol}/V_{H2O}$) were investigated in detail in order to obtain the stable PAL/CR-X-GRL@SiO_2 pigments. The PAL/CR-X-GRL@SiO_2 "Maya Red" pigments are very homogeneous with a purple-red hue.

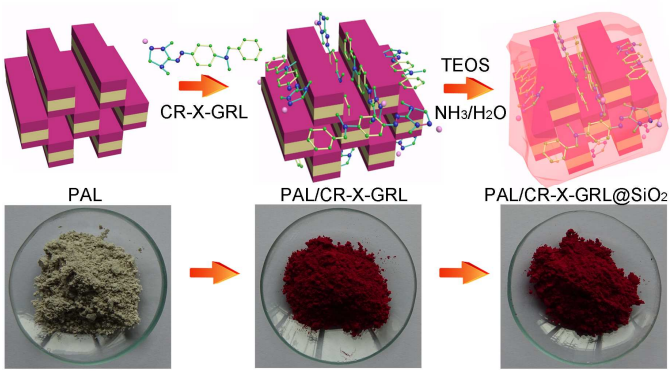

Scheme 1. Schematic illustration of preparation of the PAL/CR-X-GRL@SiO_2 "Maya Red" pigments and the corresponding images.

Preparation of PAL/CR-X-GRL pigments

The thermal stability of CR-X-GRL is low. The dark red GR-X-GRL powder became black and viscous after heated at 160 °C for 12 h as shown in Fig. 1a, b. The UV-Vis spectra of CR-X-GRL in 1 M HCl, ethanol and water are shown in Fig. 1c. All the three solutions have the maximum absorbance at 540 nm. The maximum absorbance of CR-X-GRL in water, ethanol and 1 M HCl was still at 540 nm after kept at 120 °C for 12 h, indicating that CR-X-GRL is stable under the condition (Fig. 1d). However, the characteristic absorption peak of CR-X-GRL at 540 nm disappeared after heated at 160 °C for 12 h, which means that the structure of CR-X-GRL has been changed. $m_{CR\text{-}X\text{-}GRL}/m_{PAL}$ was investigated in advance to find an appropriate CR-X-GRL content in the pigment. $m_{CR\text{-}X\text{-}GRL}/m_{PAL}$ was changed by altering the concentration of CR-X-GRL solution at a fixed solid/liquid ratio of 1/10. Fig. 2 shows UV-Vis spectra of the supernatants after adsorption, concentrations of original CR-X-GRL solution and residual CR-X-GRL in the supernatants with an $m_{CR\text{-}X\text{-}GRL}/m_{PAL}$ of 4% ~ 20%. The supernatants after adsorption are almost colourless and the absorbance of the supernatants at 540 nm is lower than 0.1 when $m_{CR\text{-}X\text{-}GRL}/m_{PAL} \leq 12\%$. The concentration of residual CR-X-GRL in the supernatants after adsorption are all about 0.012 ppm when $m_{CR\text{-}X\text{-}GRL}/m_{PAL} \leq 12\%$ although the concentration of original CR-X-GRL solution is as high as 12000 ppm. This means more than 99.9997% of CR-X-GRL was adsorbed on PAL when the concentration of CR-X-GRL is in the range of 4000 ppm to 12000 ppm. The supernatants become pink and the absorbance at 540 nm increases evidently to 0.63 corresponding to a concentration of 0.037 ppm with further increasing $m_{CR\text{-}X\text{-}GRL}/m_{PAL}$ to 20%. The concentration of residual CR-X-GRL is negligible compared with the very high original concentration. However, the existence of residual CR-X-GRL in the supernatant means there is free CR-X-GRL on the surface of the PAL/CR-X-GRL pigment, which must be removed by repeatedly washing. This procedure is time consuming and results in a large volume of wastewater. Owing to the very low residual concentration, the PAL/CR-X-GRL pigments prepared with an $m_{CR\text{-}X\text{-}GRL}/m_{PAL}$ of not more than 12% can be used directly for further tests and modification without tedious washing. The dye content in the so-obtained PAL/CR-X-GRL pigments can be as high as 12%, which is higher than all the state-of-the-art Maya Blue-like pigments. A guest molecule content, *e.g.*, indigo, of about 1% is the most frequently reported value according to the previous literatures.

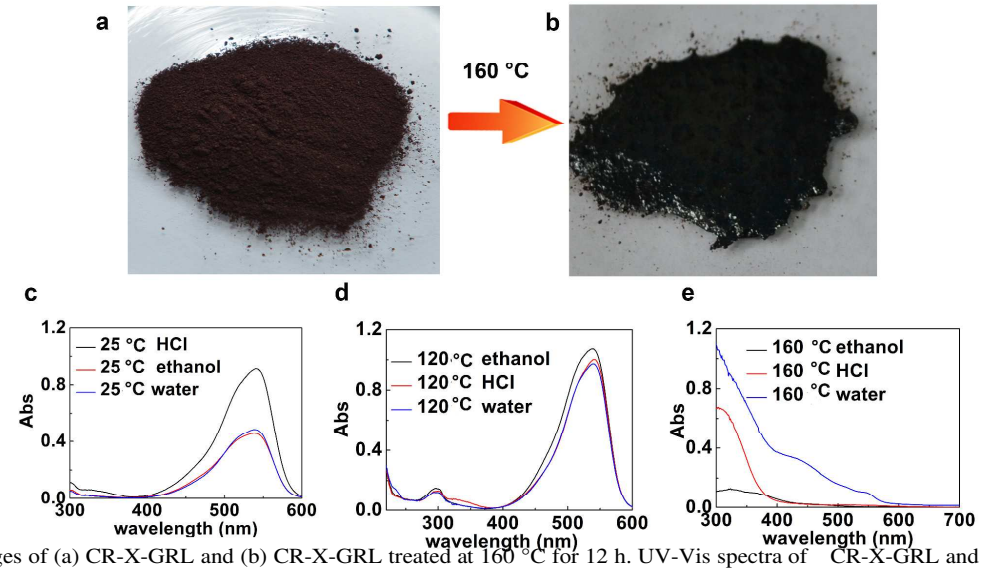

Fig. 1. Digital images of (a) CR-X-GRL and (b) CR-X-GRL treated at 160 °C for 12 h. UV-Vis spectra of CR-X-GRL and CR-X-GRL treated at (c)25 °C (d)120 °C and (e) 160 °C in 1 M HCl, ethanol and water.

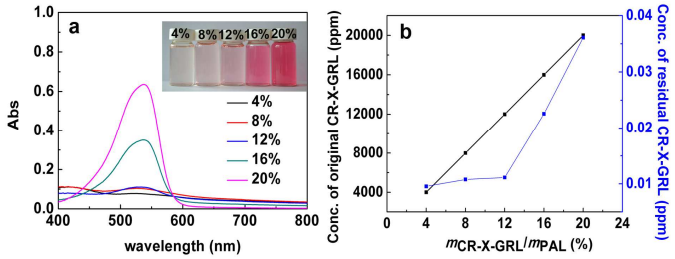

Fig. 2. (a) UV-Vis spectra of the supernatants after adsorption, (b) concentrations of original CR-X-GRL solution and residual CR-X-GRL in the supernatants with an $m_{CR\text{-}X\text{-}GRL}/m_{PAL}$ of 4% ~ 20%. The insert in (a) is the image of the supernatants after adsorption.

Solid-state grinding is a very important procedure for preparing Maya Blue-like pigments. We also studied the effect of solid-state grinding on stability of the PAL/CR-X-GRL pigments. It was found that the stability of the pigments became progressively worse in ethanol with increasing milling time (Fig. S1). This means solid-state grinding is not helpful for preparing the PAL/CR-X-GRL pigments, which makes their fabrication simpler.

It can be seen from the spectra and images of the supernatants after leaching of dye from the pigment in ethanol (Fig. S1) that the stability of the PAL/CR-X-GRL pigments is not very high although the parameters for the adsorption of CR-X-GRL have been optimized. Thus, a process of surface modification using SiO_2 is chosen to further improve stability of the pigments.

Preparation of PAL/CR-X-GRL@SiO_2 pigments

The PAL/CR-X-GRL@SiO_2 pigments were prepared by coating PAL/CR-X-GRL with a layer of SiO_2 via a modified Stöber method.[38] TEOS underwent hydrolysis and polycondensation on the surface of PAL/CR-X-GRL, and formed a layer of SiO_2 on the surface. No colour change was observed for the PAL/CR-X-GRL@SiO_2 pigments because the SiO_2 layer is transparent. The parameters influencing the polycondensation of TEOS, *e.g.*, amounts of TEOS and ammonia and $V_{ethanol}/V_{H2O}$ were investigated.

The effect of TEOS concentration on stability of the PAL/CR-X-GRL@SiO_2 pigments was studied. The UV-Vis spectra of the supernatants after attack of the pigments for 24 h using 1 M HCl, 1 M NaOH and ethanol are shown in Fig. 3a-c. Compared with the sample prepared without TEOS (PAL/CR-X-GRL), the absorbance of the supernatants decreases evidently after 1% TEOS was used to form the SiO_2 layer. This means the stability of the PAL/CR-X-GRL pigments is improved after coated with SiO_2. The silanols and siloxanes groups could form the walls of the SiO_2 glass cage during the hydrolysis and condensation of TEOS.[39] Owing to the shielding effect of SiO_2, the interaction between the pigment and the external chemicals as well as the leakage of CR-X-GRL are limited. However, the absorbance of the supernatants increases with further increasing the TEOS concentration. Too much TEOS may hinder the condensation of hydrolyzed TEOS into SiO_2 because the water content in the system is limited.

Ammonia acts as a catalyst by providing OH^- ions necessary for hydrolysis and polycondensation of TEOS.[40] A proper ammonia concentration could improve stability of the PAL/CR-X-GRL@SiO_2 pigments. Fig. 3(d) shows that the absorbance of the supernatants attacked by 1 M HCl is gradually reduced with increasing ammonia concentration to 0.8%. The lowest absorbance after attacked by 1 M NaOH and ethanol appears at an ammonia concentration of 0.6% and 0.4%, respectively. The further increase in the ammonia concentration produces an increased amount of ethanol as a byproduct, which restricts the hydrolysis and condensation of TEOS.[40]

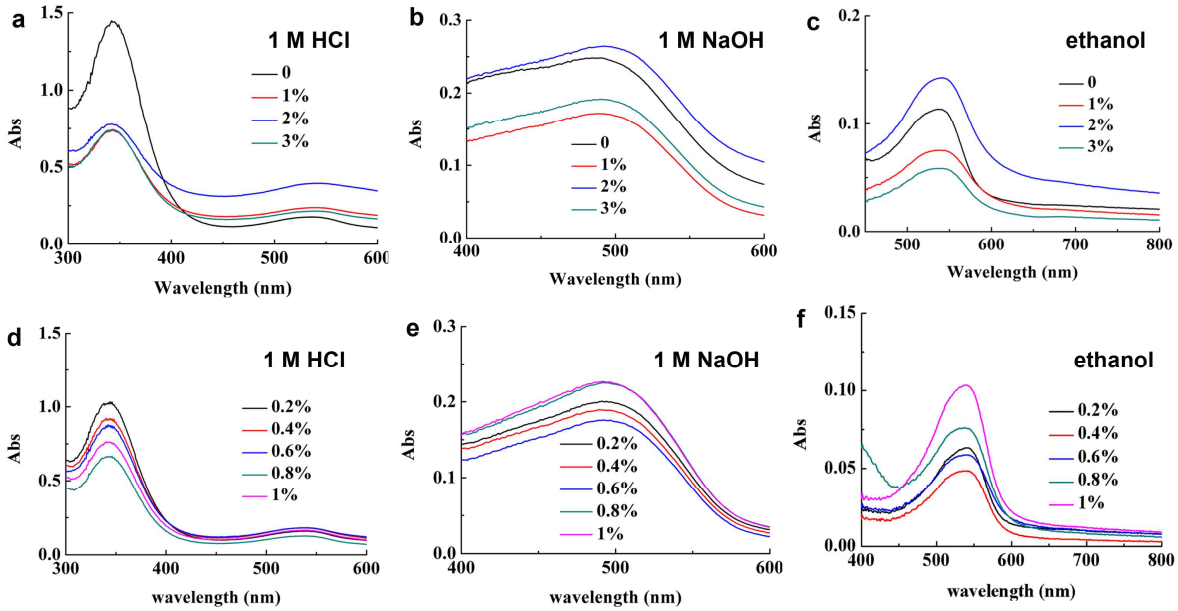

Fig. 3. Variation of UV-Vis spectra of the supernatants with (a-c) TEOS concentration and (d-f) ammonia concentration after attack of the PAL/CR-X-GRL@SiO_2 pigments using 1M HCl, 1 M NaOH and ethanol for 24 h.

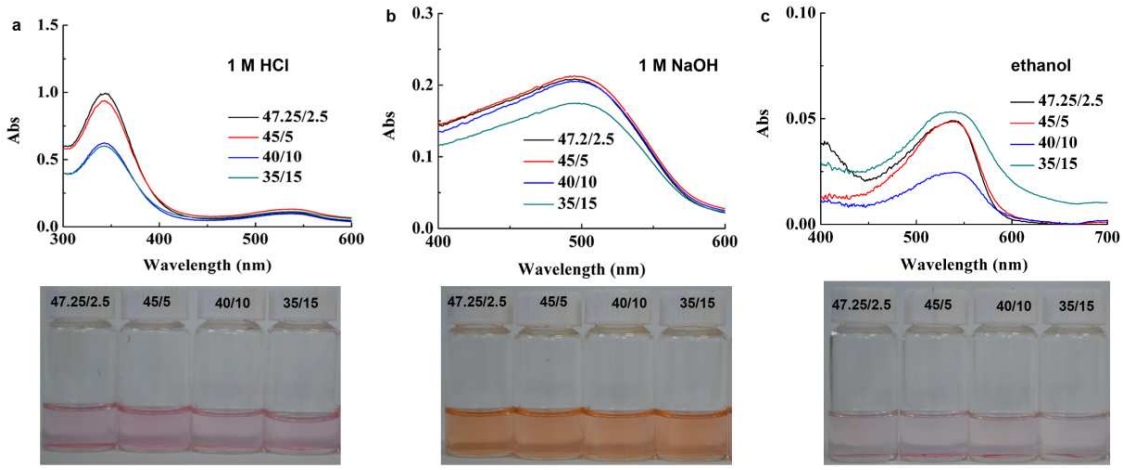

Fig. 4. Variation of UV-Vis spectra and images of the supernatants with $V_{ethanol}/V_{H2O}$ after attack of the PAL/CR-X-GRL@SiO_2 pigments using (a) 1M HCl, (b) 1M NaOH and (c) ethanol for 24 h.

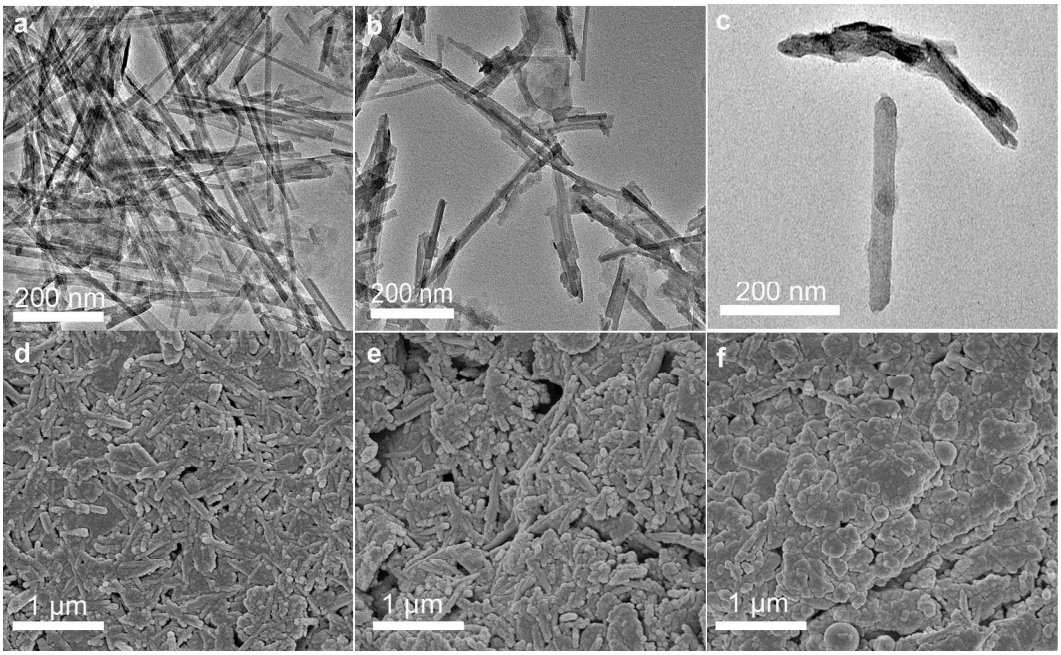

Fig. 5. TEM and SEM images of (a, d) PAL, (b, e) PAL/CR-X-GRL and (c, f) PAL/CR-X-GRL@SiO_2.

The effect of $V_{ethanol}/V_{H2O}$ on stability of the PAL/CR-X-GRL@SiO_2 pigments during preparation of the SiO_2 layer is shown in Fig. 4. Water is necessary for the hydrolysis of TEOS and higher water content could promote the hydrolysis of TEOS in ethanol. Although the images of the supernatants after attack of the PAL/CR-X-GRL@SiO_2 pigments have no difference, the absorbance of the supernatants attacked by 1 M HCl solution increases with increasing $V_{ethanol}/V_{H2O}$. The absorbance in 1 M NaOH and ethanol are pretty low and has no obvious difference. This means the sample with a $V_{ethanol}/V_{H2O}$ of 40/10 is more stable to the attack of chemicals. The hydrolysis and polycondensation of TEOS is slowly when the solvent is composed of more ethanol.[25] A proper $V_{ethanol}/V_{H2O}$ is helpful for the formation of the SiO_2 layer on the surface of the PAL/CR-X-GRL pigments, and then improves the stability.

Analyses of PAL/CR-X-GRL@SiO_2 pigments

The morphology of PAL, PAL/CR-X-GRL and PAL/CR-X-GRL@SiO_2 was analyzed by TEM and SEM. The rod-like structure of PAL is about 200 ~ 600 nm in length and 20 ~ 30 nm in diameter (Fig. 5a, d). For PAL/CR-X-GRL, the surface of the PAL crystals becomes rough and the diameter increases (Fig. 5b). These results indicate the successful binding of CR-X-GRL onto PAL. The existence of SiO_2 nanoparticles also can be seen from the TEM and SEM images of the PAL/CR-X-GRL@SiO_2 pigment (Fig. 5c, f). A comparison of the TEM and SEM images between PAL/CR-X-GRL and PAL/CR-X-GRL@SiO_2 indicates that SiO_2 nanoparticles were coated on the surface of PAL/CR-X-GRL.

The XRD patterns of PAL, PAL/CR-X-GRL and PAL/CR-X-GRL@SiO_2 are shown in Fig. S2. The peaks at 2θ = 8.3°, 19.7°, 25.4°, 27.5°, 34.6° and 42.6° in the XRD pattern of PAL are the characteristic peaks of PAL. The peak at 2θ = 8.3° (d = 1.051 nm) is attributed to the basal plane (001) of PAL.[41] The peaks at 2θ = 13.6° and 16.4° correspond to the Si-O-Si crystalline layer.[42, 43] The appearance of the diffraction peaks at 2θ = 26.5° (d = 3.36 Å) and 2θ = 31.0° (d = 2.88 Å) revealed that the PAL sample contains a trace amount of quartz and montmorillonite.[44] No obvious difference in the XRD patterns of PAL, PAL/CR-X-GRL and PAL/CR-X-GRL@SiO_2 can be observed, suggesting the crystal structure of PAL was not affected in the processes of adsorption of CR-X-GRL and subsequent condensation of TEOS.

Table 1. BET data of PAL, PAL/CR-X-GRL and PAL/CR-X-GRL@SiO_2.

Samples	S_{BET} (m^2/g)	S_{micro} (m^2/g)	S_{ext} (m^2/g)	V_{total} (cm^3/g)
PAL	262.09	92.60	169.49	0.41
PAL/CR-X-GRL	128.16	11.35	116.80	0.27
PAL/CR-X-GRL@SiO_2	143.70	3.92	139.78	0.31

The binding sites of PAL locate at the surface of the fibrous clay mineral according to Shariatmadari et al.[45] So, the surface area is an important parameter reflecting the contribution of these sites to the adsorption for dye molecules. The effects of CR-X-GRL adsorption and subsequent TEOS modification on surface area and total pore volume (V_{total}) of PAL are shown in Table 1. As can be seen in Table 1, the S_{BET} of pure PAL is 262.09 m^2/g, which decreases evidently to 128.16 m^2/g for PAL/CR-X-GRL. The S_{micro} drastically decreases from 92.60 m^2/g to 11.35 m^2/g after adsorption of CR-X-GRL, which means 87.59% decrease of the S_{micro} of PAL. Meanwhile the S_{ext} also decreases from 169.49 m^2/g to 116.80 m^2/g. According to the XRD and BET results, it can be concluded that the CR-X-GRL molecules can only be adsorbed onto the external surface, the grooves and the openings of the channels of PAL, but cannot penetrate into the channels. The adsorption of CR-X-GRL at the openings blocks the channels of PAL, which is the main reason for the drastic decrease in the S_{micro}. The adsorption of CR-X-GRL on the external surface of PAL results in the partly decrease of S_{ext} to 116.8 m^2/g. The loading of CR-X-GRL onto PAL also decreases the V_{total} from 0.41 cm^3/g to 0.27 cm^3/g. After modification with TEOS, the S_{BET} of PAL/CR-X-GRL@SiO_2 increased from 128.2 to 143.7 cm^2/g and V_{Total} increased from 0.27 to 0.32 cm^3/g. These results confirm that the silica nanoparticles are successfully coated on the surface of PAL/CR-X-GRL.

Fig. 6 shows FTIR spectra of CR-X-GRL, PAL, PAL/CR-X-GRL and PAL/CR-X-GRL@SiO_2. For CR-X-GRL, the bands at 3431 cm^{-1} and 1298 cm^{-1} are attributed to the stretching vibration of N-H and C-N groups, respectively. The bands at 1603, 1549, 1449 and 1398 cm^{-1} are attributed to the skeleton vibration of benzene of CR-X-GRL. For PAL, the bands at 3553 cm^{-1} belongs to the stretching vibration of H-O-H (crystal water), 3414 cm^{-1} is attributed to the stretching vibration of H-O-H (zeolitic water), and 1651 cm^{-1} is correspond to the bending vibration of H-O-H (crystal water and zeolitic water). The stretching vibration of Si-O-Si band is at 1028 cm^{-1} and the stretching vibration of Al-O-Si band is at 788 cm^{-1}.[46, 47] After adsorption of CR-X-GRL on PAL, the absorption bands of CR-X-GRL appear in the spectrum of PAL/CR-X-GRL, which means formation of the PAL/CR-X-GRL hybrid. The further modification of PAL/CR-X-GRL with the SiO_2 layer makes the band at 1028 cm^{-1} broader due to the overlap of Si-O-Si of SiO_2 with PAL.

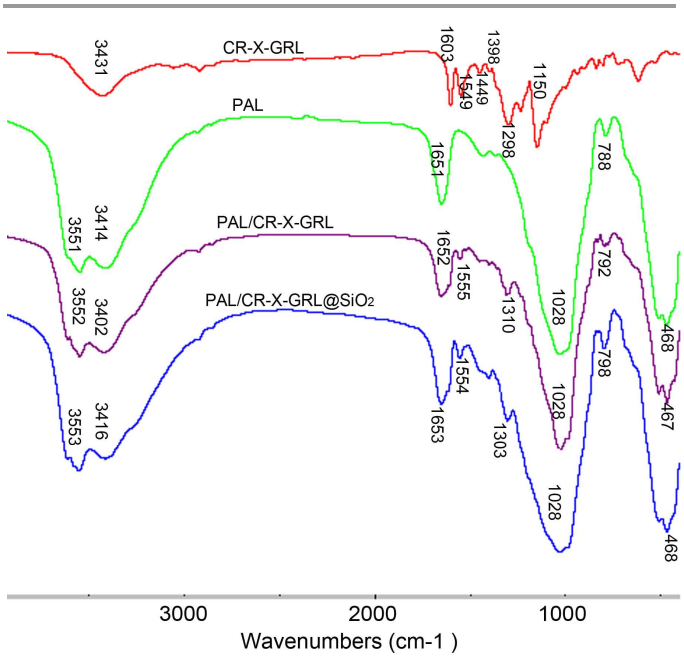

Fig. 6. FTIR spectra of CR-X-GRL, PAL, PAL/CR-X-GRL and PAL/CR-X-GRL@SiO_2.

Stability of PAL/CR-X-GRL@SiO_2 pigments

Thermal stability of organic pigments is of great importance for practical applications. The thermogravimetric analysis (TGA) of PAL, CR-X-GRL, PAL/CR-X-GRL and PAL/CR-X-GRL@SiO_2 is shown in Fig. 7. The TGA curve of PAL is consistent with previous studies[48, 49] and can be divided in four sections. The weight loss at temperature below 120 °C is attributed to desorption of loosely bound (physisorbed) water and some zeolitic water. The latter weight loss in the range of 120 °C to 300 °C is attributed to the loss of the residual zeolitic water and some weakly bound structural water molecules. The total weight loss in the first two steps is about 9%. The third weight loss in the range of 300 °C ~ 450 °C is attributed to the release of the residual structural water and the formation of PAL anhydride. The progressive weight loss was observed with further increasing the temperature to 700 °C owing to the dehydroxylation and phase transformation of PAL to clino-enstatite.[16] For CR-X-GRL, evident weight loss was observed at temperature higher than 200 °C. The total weight

loss is 48% with increasing the temperature to 800 °C. The thermal stability of the PAL/CR-X-GRL and PAL/CR-X-GRL@SiO_2 are superior to that of PAL and CR-X-GRL. The total weight loss in the range of 25 to 800 °C is in the order of CR-X-GRL > PAL > PAL/CR-X-GRL@SiO_2 > PAL/CR-X-GRL. This means the combination of CR-X-GRL and PAL greatly improved their stability. This is probably due to the fact that the opening of channels and the grooves of PAL are blocked by CR-X-GRL molecules which partly mitigates the loss of zeolitic OH_2.[24] This result is consistent with the BET and XRD analyses. For PAL/CR-X-GRL@SiO_2, the total weight loss increases to 14% and is slightly higher than that of PAL/CR-X-GRL. The more weight loss compared with PAL/CR-X-GRL might be due to the removal of some Si-OH groups of the SiO_2 nanoparticles. The major weight loss for PAL/CR-X-GRL and PAL/CR-X-GRL@SiO_2 compared with PAL is because of the degradation of CR-X-GRL.

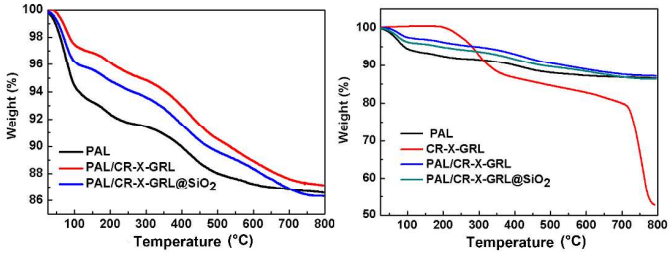

Fig. 7. TGA curves of PAL, CR-X-GRL, PAL/CR-X-GRL and PAL/CR-X-GRL@SiO_2.

The thermal stability of the pigments was also evaluated under air atmosphere (Fig. 8). As has been mentioned above, the dark red GR-X-GRL powder became black and viscous after heated at 160 °C for 12 h, whereas the PAL/CR-X-GRL pigments are very stable during the thermal stability tests under air atmosphere. The PAL/CR-X-GRL pigments remain bright purple-red after heated at 60 °C, 140 °C and 160 °C for 12 h. This result means PAL could obviously enhance thermal stability of CR-X-GRL owing to the host-guest interaction between them and the shielding effect of PAL. The further modification with silica has no influence on thermal stability of the pigments at temperature not more than 160 °C.

The PAL/CR-X-GRL and PAL/CR-X-GRL@SiO_2 pigments were immersed in 1M HCl, 1M NaOH and ethanol at room temperature for 3 d in order to track and evaluate their chemical stability. The PAL/CR-X-GRL@SiO_2 pigment shows high stability to the attack of these three chemicals. The UV–Vis spectra of the supernatants exhibit the maximum absorbance at different wavelength in 1 M HCl (350 nm), 1 M NaOH (500 nm) and ethanol (400 nm and 540 nm) as shown in Fig. 9. The supernatants of PAL/CR-X-GRL@SiO_2 pigments attacked by 1 M HCl and 1 M NaOH show obviously lower absorbance than those of the PAL/CR-X-GRL pigments. This means the PAL/CR-X-GRL@SiO_2 pigments are very stable in the acid and alkali solutions. The stability of PAL/CR-X-GRL@SiO_2 is higher than PAL/CR-X-GRL in the first day in ethanol. The further increase in immersion time results in release of a bit more dye.

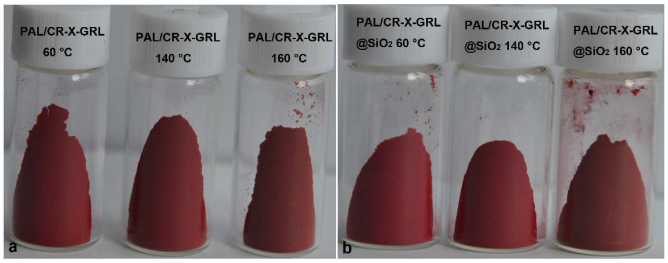

Fig. 8. Images of (a) PAL/CR-X-GRL and (b) PAL/CR-X-GRL@SiO_2 after heated at 60 °C, 140 °C and 160 °C for 12 h.

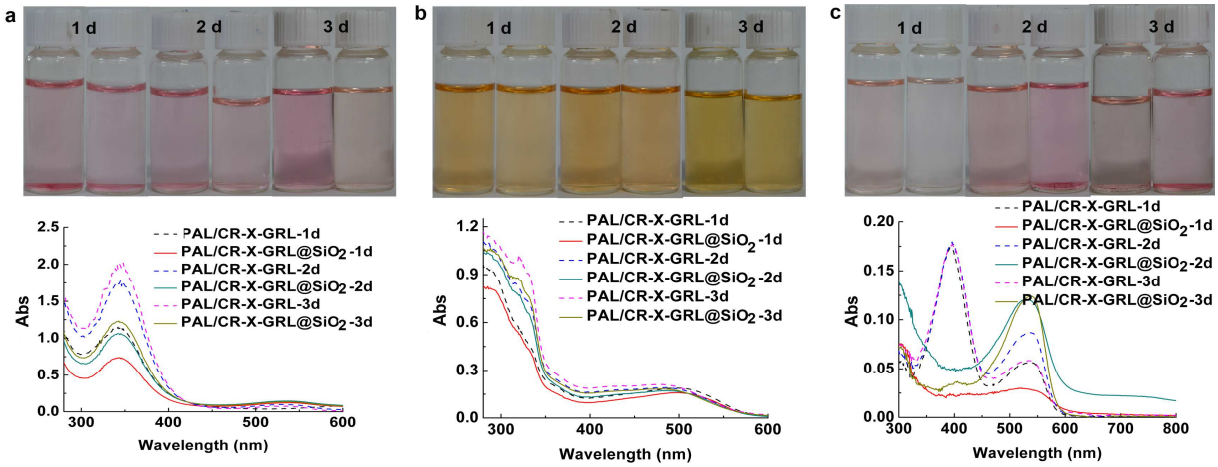

Fig. 9. UV-Vis spectra and images of the supernatants after attack of the PAL/CR-X-GRL and the PAL/CR-X-GRL@SiO_2 pigments using (a) 1M HCl, (b) 1 M NaOH and (c) ethanol for 3 d.

Fig. 10 shows SEM images of PAL/CR-X-GRL and PAL/CR-X-GRL@SiO_2 spray-coated on the aluminum foils, and the representative images of CR-X-GRL, PAL/CR-X-GRL and PAL/CR-X-GRL@SiO_2 before and after the UV irradiation tests (50 w/m^2, 60 °C). The micrographs of the spray-coated pigments are very similar to those shown in Fig. 5. CR-X-GRL is dark red before the UV accelerated weathering, whereas both PAL/CR-X-GRL and PAL/CR-X-GRL@SiO_2 are purple-red

because the silica layer is transparent.[37] CR-X-GRL and the PAL/CR-X-GRL pigment fade badly after UV irradiation for 2 d, and finally became lighter, even gray and white after continuous exposing for 3 d. For the PAL/CR-X-GRL@SiO_2 pigment, slight fading is also observable but the colour is still bright red even after UV irradiation for 3 d. The PAL/CR-X-GRL@SiO_2 pigment demonstrates higher stability to the UV accelerated weathering in comparison with CR-X-GRL and the PAL/CR-X-GRL pigment. The protective silica layer on the surface of the PAL/CR-X-GRL pigment could effectively shield the CR-X-GRL molecules in the pigment against the UV light, and then enhance the UV stability of the pigment.

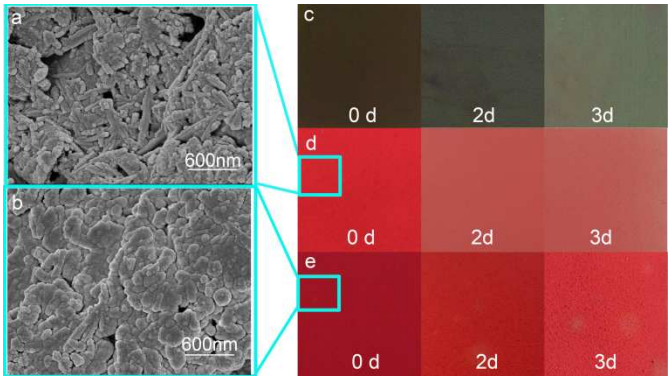

Fig. 10. SEM images of (a) PAL/CR-X-GRL and (b) PAL/CR-X-GRL@SiO_2 spray-coated on the aluminum foils, representative images of (c) CR-X-GRL, (d) PAL/CR-X-GRL and (e) PAL/CR-X-GRL@SiO_2 after UV irradiation tests for 0 d, 2 d and 3 d.

Conclusions

In summary, we reported fabrication of stable "Maya Red" pigments with purple-red hue by adsorption of CR-X-GRL onto PAL, which is followed by hydrolysis and polycondensation of TEOS via a modified Stöber method to form a layer of SiO_2. The weight ratio of CR-X-GRL to PAL in the pigments can be as high as 12%. The CR-X-GRL molecules are adsorbed onto the external surface, the grooves and the openings of the channels of PAL, but cannot enter the channels. The protective silica layer on the surface of the PAL/CR-X-GRL pigment could effectively shield the CR-X-GRL molecules in the pigment against the chemical solvents and the UV light, and then enhance stability of the pigment. The adsorption-shield of dye molecules reported herein by PAL and the silica layer may pave the way for preparing stable Maya Blue-like pigments of various colours to meet practical applications, such as pottery, statue and painting.

Acknowledgements

The authors are grateful for financial support of the "Hundred Talents Program" of the Chinese Academy of Sciences, the open funding (CASXY2013-02) the Xuyi Center of Attapulgite Applied Technology Research Development & Industrialization of the Chinese Academy of Sciences, and the Key Technology R&D Program of Jiangsu (BE2014102).

Notes and references

[a] Center of Eco-material and Green Chemistry, Lanzhou Institute of Chemical Physics, Chinese Academy of Sciences, Lanzhou, 730000, P. R. China. E-mail: jpzhang@licp.cas.cn
[b] R&D Center of Xuyi Palygorskite Applied Technology, Lanzhou Institute of Chemical Physics, Chinese Academy of Science, Lanzhou 730000, China.
[c] Graduate University of the Chinese Academy of Sciences, 100049 Beijing, P. R. China.

1. R. Fernández-Saavedra, P. Aranda and E. Ruiz-Hitzky, *Adv. Funct. Mater.*, 2004, **14**, 77.
2. G. Calzaferri, S. Huber, H. Maas and C. Minkowski, *Angew. Chem. Int. Ed.*, 2003, **42**, 3732.
3. E. Ruiz-Hitzky, *J. Mater. Chem.*, 2001, **11**, 86.
4. P. Gómez-Romero and C. Sanchez, *New J. Chem.*, 2005, **29**, 57.
5. H. Merwin, *The Temple of the warriors at Chitzen Iztá, Yucatán. Carniegie Institution of Washington Publication*, 1931, **606**.
6. M. José-Yacamán, L. Rendón, J. Arenas and M. C. S. Puche, *Science*, 1996, **273**, 223.
7. R. Giustetto, O. Wahyudi, I. Corazzari and F. Turci, *Appl. Clay Sci.*, 2011, **52**, 41.
8. A. Tilocca and E. Fois, *J. Phys. Chem. C*, 2009, **113**, 8683.
9. S. Yariv and H. Cross, *Organo-clay complexes and interactions*, CRC Press, 2001.
10. E. Ruiz-Hitzky, P. Aranda, M. Darder and G. Rytwo, *J. Mater. Chem.*, 2010, **20**, 9306.
11. H. Van Olphen, *Science*, 1966, **154**, 645.
12. A. Doménech, M. T. Doménech-Carbó and M. L. Vázquez de Agredos-Pascual, *Angew. Chem. Int. Ed.*, 2011, **50**, 5741.
13. A. Doménech, M. T. Doménech-Carbó, C. Vidal-Lorenzo and M. L. V. de Agredos-Pascual, *Angew. Chem. Int. Ed.*, 2012, **51**, 700.
14. G. Chiari, R. Giustetto and G. Ricchiardi, *Eur. J. Minera.*, 2003, **15**, 21.
15. E. Fois, A. Gamba and A. Tilocca, *Micro. Meso. Mater.*, 2003, **57**, 263.
16. R. Giustetto, F. Xamena, G. Ricchiardi, S. Bordiga, A. Damin, R. Gobetto and M. R. Chierotti, *J. Phys. Chem. B*, 2005, **109**, 19360.
17. G. Chiari, R. Giustetto, J. Druzik, E. Doehne and G. Ricchiardi, *Appl. Phys. A*, 2008, **90**, 3.
18. M. S. del Río, E. Boccaleri, M. Milanesio, G. Croce, W. van Beek, C. Tsiantos, G. D. Chyssikos, V. Gionis, G. H. Kacandes and M. Suárez, *J. Mater. Sci.*, 2009, **44**, 5524.
19. M. Sánchez del Río, E. Boccaleri, M. Milanesio, G. Croce, W. van Beek, C. Tsiantos, G. Chyssikos, V. Gionis, G. Kacandes, M. Suárez and E. García-Romero, *J. Mater. Sci.*, 2009, **44**, 5524.
20. B. Hubbard, W. Kuang, A. Moser, G. A. Facey and C. Detellier, *Clays Clay Miner.*, 2003, **51**, 318.
21. Y. Nagasawa, R. Taguri, H. Matsuda, M. Murakami, M. Ohama, T. Okada and H. Miyasaka, *Phys. Chem. Chem. Phys.*, 2004, **6**, 5370..
22. A. Domenech-Carbo, M. Teresa Domenech-Carbo, F. Manuel Valle-Algarra, M. E. Domine and L. Osete-Cortina, *J. Mater. Sci.*, 2013, **48**, 7171..
23. A. Domenech-Carbo, F. M. Valle-Algarra, M. T. Domenech-Carbo, M. E. Domine, L. Osete-Cortina and J. V. Gimeno-Adelantado, *ACS Appl. Mater. Interfaces*, 2013, **5**, 8134.

24. R. Giustetto, F. X. Llabrés i Xamena, G. Ricchiardi, S. Bordiga, A. Damin, R. Gobetto and M. R. Chierotti, *J. Phys. Chem. B*, 2005, **109**, 19360.
25. C. Mondelli, M. S. d. Río, M. A. González, A. Magazzú, C. Cavallari, M. Suárez, E. García-Romero and P. Romano, *J. Phys. Conference Series*, 2012, **340**, 012109.
26. E. Lima, A. Guzmán, M. Vera, J. L. Rivera and J. Fraissard, *J. Phys. Chem. C*, 2012, **116**, 4556.
27. M. M. Lezhnina, T. Grewe, H. Stoehr and U. Kynast, *Angew. Chem. Int. Ed.*, 2012, **51**, 10652..
28. R. Giustetto, K. Seenivasan, D. Pellerej, G. Ricchiardi and S. Bordiga, *Micro. Meso. Mater.*, 2012, **155**, 167.
29. R. Giustetto and O. Wahyudi, *Micro. Meso. Mater.*, 2011, **142**, 221..
30. S. Islam, R. Rahman, Z. Othaman, S. Riaz and S. Naseem, *J. Ind. Eng. Chem.*, 2014. In press.
31. S. Bonacchi, D. Genovese, R. Juris, M. Montalti, L. Prodi, E. Rampazzo and N. Zaccheroni, *Angew. Chem. Int. Ed.*, 2011, **50**, 4056.
32. R. Pardo, M. Zayat and D. Levy, *Chem. Soc. Rev.*, 2011, **40**, 672.
33. N. J. Halas, *ACS Nano*, 2008, **2**, 179.
34. X. Zhao, L. R. Hilliard, K. Wang and W. Tan, *Encyclopedia Nanoscience Nanotechnology*, 2004, **1**, 255.
35. L. Wang, K. Wang, S. Santra, X. Zhao, L. R. Hilliard, J. E. Smith, Y. Wu and W. Tan, *Anal. Chem.*, 2006, **78**, 646.
36. Y. Jin, S. Kannan, M. Wu and J. X. Zhao, *Chem. Res. Toxicol.*, 2007, **20**, 1126.
37. D. M. Liu and I. Chen, *Acta Mater.*, 1999, **47**, 4535.
38. W. Stöber, A. Fink and E. Bohn, *J. Colloid Interf. Sci.*, 1968, **26**, 62.
39. K. K. Unger, *Porous silica*, Elsevier, 1979.16.
40. R. P. Bagwe, C. Yang, L. R. Hilliard and W. Tan, *Langmuir*, 2004, **20**, 8336.
41. Q. Fan, D. Shao, J. Hu, W. Wu and X. Wang, *Surf. Sci.*, 2008, **602**, 778.
42. E. Cao, R. Bryant and D. J. Williams, *J. Colloid Interf. Sci.*, 1996, **179**, 143.
43. D. Zhao, J. Zhou and N. Liu, *Mater. Charact.*, 2007, **58**, 249.
44. G. Brown and G. Brindley, *Mineralog. Soc., London*, 1980, 361.
45. L. G. Cecil, *J. Archaeol. Sci.*, 2010, **37**, 1006.
46. M. Suárez and E. Garcia-Romero, *Appl. Clay Sci.*, 2006, **31**, 154.
47. L. A. Polette-Niewold, F. S. Manciu, B. Torres, M. Alvarado, Jr. and R. R. Chianelli, *J. Inorg. Biochem.*, 2007, **101**, 1958.
48. J. Xu, W. Wang and A. Wang, *Powder Technol.*, 2013, **235**, 652.
49. R. L. Frost and Z. Ding, *Thermochim. Acta*, 2003, **397**, 119.